The Journal of
Eukaryotic Microbiology

Published by the International Society of Protistologists

Journal of Eukaryotic Microbiology ISSN 1066-5234

ORIGINAL ARTICLE

Schmidingerothrix salinarum nov. spec. is the Molecular Sister of the Large Oxytrichid Clade (Ciliophora, Hypotricha)

Wilhelm Foissner[a], Sabine Filker[b] & Thorsten Stoeck[b]

a Department of Organismic Biology, University of Salzburg, Hellbrunnerstrasse 34, A-5020 Salzburg, Austria
b Department of Ecology, University of Kaiserslautern, Erwin-Schrödingerstrasse 14, D-67663 Kaiserslautern, Germany

Keywords
Ancestral hypotricha; biodiversity; hypersaline habitats; Portugal; solar saltern.

Correspondence
W. Foissner, Universität Salzburg, Fachbereich Organismische Biologie, Hellbrunnerstrasse 34, A-5020 Salzburg, Austria
Telephone number: +43(0)662-8044-5615; FAX number: +43(0)662-8044-5698; e-mail: wilhelm.foissner@sbg.ac.at

Received: 3 May 2013; revised 23 September 2013; accepted September 24, 2013.

doi:10.1111/jeu.12087

ABSTRACT

In 2012, Foissner described a curious hypotrich: *Schmidingerothrix extraordinaria*. This ciliate, which he discovered in hypersaline soils (~100‰) from Namibia, had a frayed buccal lip, three-rowed adoral membranelles, only one frontal cirrus, and a miniaturized first frontal membranelle, while a paroral membrane, dorsal bristle rows and buccal, transverse and caudal cirri were absent. All opisthe structures developed de novo, while parental structures were involved in the proter. When Foissner's study became available, we discovered a similar species in a Portuguese solar saltern, differing from *S. extraordinaria* mainly by the number of frontoventral cirral rows (3 vs. 1). Furthermore, parental structures were involved in the ontogenesis of both proter and opisthe. The small subunit (SSU) rDNA shows *Schmidingerothrix* as sister of a large clade containing most classical oxytrichids (e.g. *Sterkiella, Oxytricha, Steinia*) and many related taxa (e.g. *Pattersoniella, Bistichella, Uroleptus*). This clade shows a bifurcation named "*Oxytricha* subclade" and "*Uroleptus* subclade". Foissner (2012) interpreted the peculiarities of *Schmidingerothrix* as a reduction caused by the extreme habitat. However, the molecular data do not exclude that *Schmidingerothrix* presents an ancient state. A morphology-based scheme is presented, showing how the subclades might have evolved from a *Schmidingerothrix*-like ancestor.

RECENT molecular and morphological investigations greatly contributed in understanding evolution and phylogeny of the hypotrichs (Berger 2008; Foissner et al. 2004; Hu et al. 2011; Liu et al. 2010; Paiva et al. 2009; Schmidt et al. 2007). These studies showed a basal dichotomy of the Euplota and of the Hypotricha as well as a widespread occurrence of homoplasies affecting even "strong" morphological characters, such as the midventral cirral and the dorsal bristle pattern, making the relationships within the Hypotricha very complex. For instance, species with a "typical" *Oxytricha* cirral pattern appear in six clades of the molecular trees (Foissner et al. 2004; this study, Fig. 5). Thus, Berger (2008) suggested an *Oxytricha*-like ciliate with 18 fronto-ventral-transverse cirri, 3 caudal cirri, and 3 dorsal bristle rows as last common ancestor of the Hypotricha.

However, in 2012, Foissner described *Schmidingerothrix extraordinaria*, a very curious hypotrich without dorsal bristle rows that are possibly the most characteristic plesiomorphy of the Hypotricha and Euplota. Thus, Foissner (2012) concluded: "*Schmidingerothrix extraordinaria* is very likely a secondarily oligomerized hypotrich, and the reduction occurred possibly very long ago because no traces of the ancestral ciliature remained in the ontogenetic processes. Possibly, the simple ciliature is an adaptation to highly saline habitats, where competition is low and bacterial food abundant."

Foissner (2012) did not have a molecular sequence of *Schmidingerothrix*. Thus, we were electrified when we found a *Schmidingerothrix*-like ciliate in a solar saltern of the Ria Formosa Natural Park (Faro, Portugal). Silver impregnation of the this ciliate showed indeed a close morphological similarity with *S. extraordinaria*, and the ribosomal gene sequences place it as a sister to a large clade containing both, most classical oxytrichids (e.g., *Oxytricha*, *Stylonychia*, *Steinia*) and many other taxa (e.g., *Pattersoniella*, *Bistichella*, *Engelmanniella*).

MATERIAL AND METHODS

Material

Schmidingerothrix salinarum was discovered in a solar saltern pond of the Ria Formosa Natural Park, close to the town of Faro, Portugal, N 37°0′29.4851″, W 7°57′

41.0684″. It could be cultivated on sterilized artificial sea water (Instant Ocean, Aquarium Systems, Mentor OH, 12%) amended with one wheat grain per 25 ml of culture to support growth of indigenous bacteria.

Morphological methods

All data are from cultivated specimens. Living cells were studied using a high-power oil immersion objective and differential interference contrast microscopy. Protargol impregnation and scanning electron microscopy (SEM) were performed as described by Vd'ačný and Foissner (2012). Some drops of osmium acid (2%) were added to Stieve's solution to obtain well-fixed cells; in spite of this, the cells became inflated (width) and shrunk (length) by about 20%. The nuclear apparatus was stained with hematoxylin, using a histological standard protocol (Adam and Czihak 1964).

Counts and measurements of silvered specimens were performed at a magnification of 1,000×. In vivo measurements were conducted at magnifications of 40–1,000×. Drawings of live specimens were based on free-hand sketches and micrographs; those of impregnated cells were made with a drawing device. In the ontogenetic stages, parental structures are shown by outline, while newly formed structures are shaded black. Each of the stages depicted has been seen in at least two specimens.

Molecular and phylogenetic methods

DNA extraction, PCR amplification of the small subunit rDNA (SSU rDNA), and phylogenetic analyses were conducted as described previously (Foissner and Stoeck 2011). In short, genomic DNA was extracted from 10 specimens of *Schmidingerothrix salinarum* using the DNEasy Tissue Kit (Qiagen, Hilden, Germany) and the SSU rDNA was amplified using the universal eukaryotic primers EukA and EukB (Medlin et al. 1988). Amplification: 5 min at 95 °C followed by 30 identical amplification cycles of denaturation at 95 °C for 45 s, annealing at 55 °C for 1 min, and extension at 72 °C for 2.5 min, and a final extension at 72 °C for 7 min. The purified PCR product (MiniElute kit, Qiagen) was cloned into a vector using the TA-Cloning Kit (Invitrogen, Carlsbad, CA). M13F and M13R sequences were obtained with the Big Dye Terminator Kit (Applied Biosystems, Foster City, CA) on an ABI 3730 automated sequencer and assembled in CodonCode Aligner (CodonCode Corporation, Centerville, MA).

For assessment of the phylogenetic placement of *S. salinarum*, its 18S rDNA sequence was aligned to homologous sequences of hypotrich ciliates available in GenBank, including sequences of the closest described relatives of *S. salinarum,* deposited in this database. As outgroup, we chose representative sequences from choreotrich and

Table 1. GenBank accession numbers of sequences used for phylogenetic analyses (Fig. 5) in this study

Taxa	Accession number	Taxa	Accession number
Amphisiella magnigranulosa	AM412774.1	*Oxytricha longa*	AF164125.1
Apobakuella fusca	JN008942.1	*Oxytricha saltans*	AF370028.1
Aspidisca steini	AF305625.1	*Parabirojimia similis*	DQ503584.1
Bistichella variabilis	HQ699895.1	*Parabistichella variabilis*	JN008943.1
Cyrtohymena citrina	AF164135.1	*Paradiscocephalus elongatus*	EU684746.1
Diaxonella pseudorubra	GU942564.1	*Parasterkiella thompsoni*	HM569264.1
Diophrys oligothrix	DQ353850.1	*Paraurostyla viridis*	AF508766.1
Engelmanniella mobilis	AF508757.1	*Paruroleptus lepisma*	AF164132.1
Epiclintes auricularis rarisetus	FJ008722.1	*Pattersoniella vitiphila*	AJ310495.1
Euplotidium arenarium	Y19166.1	*Plagiotoma lumbrici*	AY547545.1
Eutintinnus pectinis	JN831766.1	*Pleurotricha lanceolata*	FJ748886.1
Gastrostyla steinii	AF164133.1	*Salpingella acuminata*	EU399536.1
Gonostomum namibiense	AY498655.1	*Schmidingerothrix salinarum*	KC991098
Halteria grandinella	AF194410.1	*Steinia sphagnicola*	AJ310494.1
Hemicycliostyla sphagni	FJ361758.1	*Sterkiella cavicola*	GU942565.1
Hemigastrostyla enigmatica	EF194085.1	*Strobilidium caudatum*	AY143573.1
Hemiurosoma terricola	AY498651.1	*Strombidium purpureum*	U97112.1
Kahliella sp. TT2005	EU079472.1	*Strongylidium pseudocrassum*	DQ910903.2
Laurentiella strenua	AJ310487.1	*Stylonychia mytilus*	AF508774.1
Meseres corlissi	EU399528.1	*Stylonychia notophora*	FM209297.1
Neokeronopsis aurea	EU124669.1	*Stylonychia pustulata*	X03947.1
Novistrombidium orientale	FJ422988.1	*Tintinnidium mucicola*	AY143563.1
Onychodromopsis flexilis	AY498652.1	*Tunicothrix wilberti*	GU437210.1
Orthoamphisiella breviseries	AY498654.1	*Uroleptopsis citrina*	FJ870094.1
Oxytricha elegans	AM412767.1	*Uroleptus gallina*	AF164130.1
Oxytricha ferruginea	AF370027.1	*Uroleptus pisces*	AF164131.1
Oxytricha granulifera	AM412771.1	*Uronychia setigera*	JF694042.1
Oxytricha lanceolata	AM412773.1	*Urostyla grandis*	AF164129.1

oligotrich ciliates (Table 1). Alignments were constructed in the Seaview program package (vers. 4.2, Galtier et al. 1996) using Muscle (Edgar 2004) and uninformative and ambiguous positions were identified and excluded using Gblocks (Castresana 2000).

The resulting alignment included 1,686 characters from 56 taxa and is available by the authors upon request. The GTR-I-Γ evolutionary model was the best fitted model selected by the AIC in jModeltest v0.1.1 (Guindon and Gascuel 2003; Posada 2008). Evolutionary distance (ED) and maximum-likelihood (ML) analyses were conducted for phylogenetic placement of *S. salinarum*. Neighbor-joining ED analysis was carried out in the Seaview program package (vers. 4.2, Galtier et al. 1996). ML bootstrapping analyses were carried out with 100 replicates using RAxML with the setting as described in Stamatakis et al. (2008). We consider NJ and ML bootstrap support > 75 as strong and > 95 as significant. Values < 50 are unsupported nodes. Tree interpretation follows Krell and Cranston (2004) and Crisp and Cook (2005). The GenBank accession number of *S. salinarum* is KC991098.

Terminology

For general and specific terms, see Lynn (2008) and Berger (2011). Details of the oral apparatus are according to Foissner and Al-Rasheid (2006).

RESULTS

Description of *S. salinarum* nov. spec. (Table 2 and Fig. 1A–L, 2–5)

Schmidingerothrix salinarum has a size of 70–110 × 15–25 μm in vivo, usually it is 95 × 17 μm, as calculated from some in vivo measurements and the morphometric data shown in Table 1, adding 15% for length preparation shrinkage. The length: width ratio is 5.6:1 in vivo, whereas 4.9:1 in the protargol preparations and 4.6:1 in the SEM specimens, showing a rather strongly inflation of the cells due to the preparation procedures (Table 2).

Schmidingerothrix salinarum is highly flexible and shows a variety of shapes, of which those shown in Fig. 1A, B, H, 2B, C, E, G–K are most common, i.e., it is oblong to slightly sigmoidal and more or less coiled; the ventral margin is frequently convex, the dorsal one is slightly concave, and it is unflattened or slightly flattened laterally. The anterior body end is transversely truncate or slightly convex and has a distinct ventral indentation causing a gap separating frontal and ventral adoral membranelles. The posterior end is always acute and thus forms a short tail, usually well-recognizable also in preparations (Fig. 1A, C–E, H, K, 2F, G, I, L, 3C).

The nuclear apparatus is right of body's midline in the central sixths of the cell and is composed of three to six, usually four macronuclear nodules and zero to two micronuclei (Table 2 and Fig. 1A, C–E, 4C, H). The macronuclear nodules are broadly to slenderly ellipsoidal and impregnate only very lightly with the protargol method used, both in morphostatic and dividing cells. The micronuclei are not recognizable or absent in about one third of the specimens; in the others, there are one to two micronuclei attached or near to the macronuclear nodules. The shape is highly variable: globular, comma-shaped, or elongate reniform. A contractile vacuole is not recognizable.

The cortex is very flexible and difficult to preserve (see Methods section). It contains loose rows of colorless granules about 1 μm across (Fig. 1B); rarely, the granules impregnate with the protargol method used. The cytoplasm is colorless and contains some crystals 1–3 μm in size and innumerable, pale granules (Fig. 1A, 2D, F). *Schmidingerothrix salinarum* feeds on minute, very slender bacterial rods digested in food vacuoles 5–8 μm across. In cultures, it ingests also starch grains up to 10 μm across (Fig. 2F, K). Most specimens contain bright, possibly empty vacuoles 5–8 μm across (Fig. 1A, 2A–C, E, F, I–K). *Schmidingerothrix salinarum* swims and creeps rapidly and continuously, usually accumulating around the wheat kernels.

The cirri are 10–13 μm long in vivo, most are composed of four, rarely of two or six cilia. The cirral pattern is comparatively simple because buccal, transverse, and caudal cirri as well as dorsal bristle rows are absent (Table 2 and Fig.1A, I–L, 2G, H, 3A–D). There are two marginal cirral rows, three frontoventral cirral rows, and three frontal cirri. The marginal and frontoventral cirral rows extend helically from the right anterior to the left posterior body margin, usually slightly spreading onto the dorsal surface. The first frontoventral cirral row is short rarely extending posterior to the distal end of the endoral membrane; row 2 is as long as the body and distinctly coiled; row 3 is highly variable in length and when it is short, difficult to recognize because it is on the right body margin; rather, frequently, it has an equatorial portion composed of about five cirri (Fig. 7E). Of 87 specimens analyzed, row 3 is short and confined to the oral area in 66 (76%) specimens; is in two portions in 18 (~21%) cells; and is about as long as row 2 in three (~3%) specimens. The first and second frontal cirrus consists of six, rarely of only four cilia, the first is far subapical close to the anterior ventral portion of the adoral zone; the third frontal cirrus is composed of only four cilia and is right of the frontal adoral membranelles.

The oral apparatus is in the left anterior quadrant of the cell. It is rather inconspicuous but full of remarkable details (Table 2 and Fig.1A, I, K, 2A–E, G–K, M, 3A–C, 4A, C). The adoral zone of membranelles extends over 32% of body length on average and is composed of three frontal and 18–22 ($\bar{x}$ 21) ventral membranelles, both separated by a rather wide gap. The bases of the largest membranelles are about 4 μm wide. The individual membranelles are composed of two long and one very short row (Fig. 1I). The cilia of frontal membranelle 1 are about 10 μm long in vivo, those of membranelles 2 and 3 are about 15 μm long. The cilia of the ventral

Table 2. Morphometic data on *Schmidingerothrix salinarum*

Characteristics[a]	Mean	M	SD	SE	CV	Min	Max	*n*
Body, length (with tail) (μm)	81.6	83.0	7.7	1.7	9.4	68.0	93.0	21
Body, width (μm)	17.3	18.0	3.5	0.8	20.3	12.0	23.0	21
Body length:width, ratio in vivo (IV)	5.6	5.6	0.6	0.1	10.4	4.5	7.1	33
Body length:width, ratio in SEM	4.6	4.5	0.7	0.2	14.4	3.5	5.6	10
Body length:width, ratio	4.9	4.8	0.9	0.2	18.1	3.7	7.1	21
Anterior body end to frontal cirrus 1, distance (μm)	6.4	7.0	0.9	0.2	14.4	4.0	8.0	21
Anterior body end to endoral membrane, distance (μm)	12.7	13.0	1.4	0.3	10.9	10.0	15.0	21
Endoral membrane, length	12.0	12.0	1.9	0.4	15.7	8.0	15.0	21
Anterior body end to posterior end of V1, distance (μm)	13.2	13.0	1.6	0.4	12.4	10.0	18.0	21
Anterior body end to posterior end of V2, distance (μm)	61.4	60.0	6.6	1.4	10.7	50.0	73.0	21
Anterior body end to posterior end of V3, distance (μm)	26.2	19.0	–	–	–	7.0	73.0	21
Anterior body end to macronucleus, distance (μm)	10.1	10.0	2.0	0.4	19.3	7.0	14.0	21
Anterior body end to posterior end of adoral zone of membranelles, distance (μm)	26.5	26.0	2.5	0.5	9.3	22.0	33.0	21
Largest adoral membranelle, length of base (μm)	4.3	4.0	–	–	–	4.0	5.0	21
Anterior body end to macronucleus, distance (H) (μm)	13.5	13.0	2.4	0.5	18.0	10.0	20.0	29
Nuclear figure, length (H) (μm)	45.2	45.0	9.8	1.8	21.7	27.0	62.0	29
First macronuclear nodule, length (H) (μm)	10.5	10.0	2.4	0.5	23.1	5.0	18.0	29
First macronuclear nodule, width (H) (μm)	4.0	4.0	0.6	0.1	16.0	3.0	6.0	29
Macronuclear nodules, number (H)	4.2	4.0	0.6	0.1	14.7	3.0	6.0	29
Micronuclei, length (H) (μm)	3.2	3.0	0.4	0.1	12.1	2.5	4.0	29
Micronuclei, width (H) (μm)	2.1	2.0	0.3	0.1	15.1	1.5	3.0	29
Micronuclei, number (H)	1.4	1.0	–	–	–	1.0	2.0	29
Frontoventral cirral rows, number	3.0	3.0	0.0	0.0	0.0	3.0	3.0	29
Ventral row 1, number of cirri	4.1	4.0	0.7	0.2	18.3	2.0	5.0	21
Ventral row 2, number of cirri	17.5	18.0	2.1	0.5	12.1	12.0	20.0	21
Ventral row 3, number of cirri	5.3	5.0	2.5	0.6	47.9	2.0	12.0	21
Right marginal row, number of cirri	23.4	23.0	2.6	0.6	11.1	21.0	31.0	21
Left marginal row, number of cirri	17.5	17.0	2.0	0.4	11.2	14.0	23.0	21
Frontal cirri, number	3.0	3.0	0.0	0.0	0.0	3.0	3.0	21
Frontal adoral membranelles, number	3.0	3.0	0.0	0.0	0.0	3.0	3.0	21
Ventral adoral membranelles, number	20.8	21.0	1.1	0.3	5.4	18.0	22.0	21
Resting cyst, length with external wall (IV) (μm)	28.7	29.0	1.6	0.4	5.5	26.0	32.0	15
Resting cyst, width with external wall (IV) (μm)	28.3	28.0	1.6	0.4	5.6	27.0	31.0	15
Resting cyst, length without external wall (IV) (μm)	24.7	25.0	1.3	0.3	5.2	23.0	27.0	15
Resting cyst, width without external wall (IV) (μm)	24.2	24.0	1.3	0.3	5.2	21.0	26.0	15
Resting cyst, macronucleus length (μm)	10.4	10.0	2.2	0.6	21.4	8.0	15.0	13
Resting cyst, macronucleus width (μm)	6.5	6.0	1.4	0.4	21.5	4.9	9.0	13

CV = coefficient of variation in %; H = hematoxylin staining; IV = in vivo; mean = arithmetic mean; M = median; Max = maximum; Min = minimum; *n* = number of specimens investigated; SD = standard deviation; SE = standard error of mean; SEM = scanning electron microscopy; V = ventral cirral row.

[a]Data based, if not mentioned otherwise, on protargol-impregnated, well-preserved specimens from a single culture.

membranelles decrease in length from about 10 μm anteriorly to 4 μm posteriorly and in the right half of the membranellar stripe (Fig. 4A). The buccal cavity and the ventral adoral membranelles are covered by a convex, about 5-μm-wide buccal lip, having about 10 fringes in the posterior quarter. The fringes are about 1 μm long and can beat up and down (Fig. 1A, 2D, G, M, 4A). The buccal cavity is narrow in vivo, while usually widened in protargol and SEM preparations (Fig. 1A, K, 3B, C, 4A). The endoral membrane, which is entirely covered by the buccal lip and the buccal seal, is composed of a row of about 20 short cilia. A paroral membrane is absent. The cytopharynx is of ordinary size and limited by fibers originating from the proximal adoral membranelles and the posterior third of the endoral membrane (Fig. 1A, I, K, 3B).

The globular resting cysts are on average 28 μm across in vivo (Table 2). The cyst wall is smooth (Fig. 4G), but in old cysts, it is usually heavily colonized by bacteria. The wall is composed of an about 1-μm-thick, compact external layer (ectocyst?) and an about 0.5-μm-thick internal layer (endocyst?) not recognizable in squashed cysts (Fig. 4F). The external and the internal layer are separated by a 1- to 3-μm-thick, bright zone, possibly the mesocyst (Table 1 and Fig. 4D, 7I). The cytoplasm is studded with 0.5- to 2-μm-sized granules (lipid droplets?).

About 2% (*n* = 100) of the specimens were homopolar doublets of type I, e.g., only one oral apparatus is visible

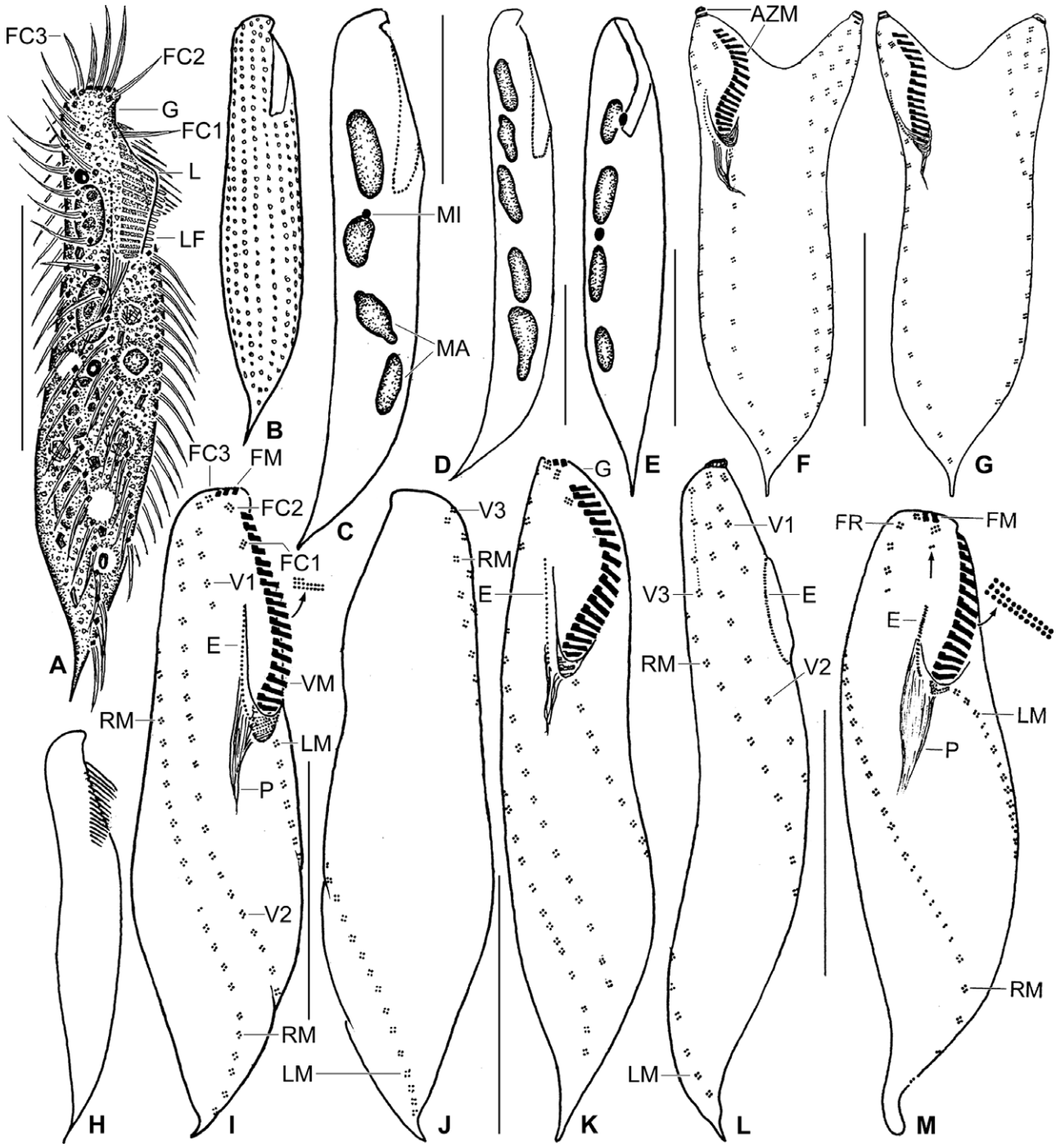

Figure 1 **(A–M)** *Schmidingerothrix salinarum* n. spec. (A–L) and *S. extraordinaria* (M, from Foissner 2012) from life (A, B, H), hematoxylin stained (C–E), and protargol-impregnated (C–G, I–M). **A.** Right side view of a representative specimen, length 100 μm. The lip (L) covers the ventral portion of the adoral membranelles. **B.** Cortical granulation (slightly schematized). **C–E, H.** Variability in body shape and nuclear apparatus. **F, G.** About 2% of the specimens are doublets. **I, J.** Right and left side view of the holotype specimen, length 75 μm. Note the absence of dorsal bristles, transverse and caudal cirri, and of a paroral membrane. The adoral membranelles are composed of only three rows of cilia (vs. four rows in most hypotrichs). **K.** Ventral view of oral and somatic infraciliature. **L.** Right lateral view, showing ventral cirral row 3. **M.** Right side view of holotype specimen of *S. extraordinaria*, which has only one frontoventral cirral row. AZM = adoral zone of membranelles; E = endoral membrane; FC1-3 = frontal cirri; FM = frontal adoral membranelles; FR = frontal cirral row; G = gap between frontal and ventral adoral membranelles; L = buccal lip; LM = left marginal cirral row; MA = macronuclear nodules; MI = micronuclei; P = pharynx; RM = right marginal cirral row; V1-3 = frontoventral cirral rows. Scale bars 30 μm (C–G, J–M) and 40 μm (A).

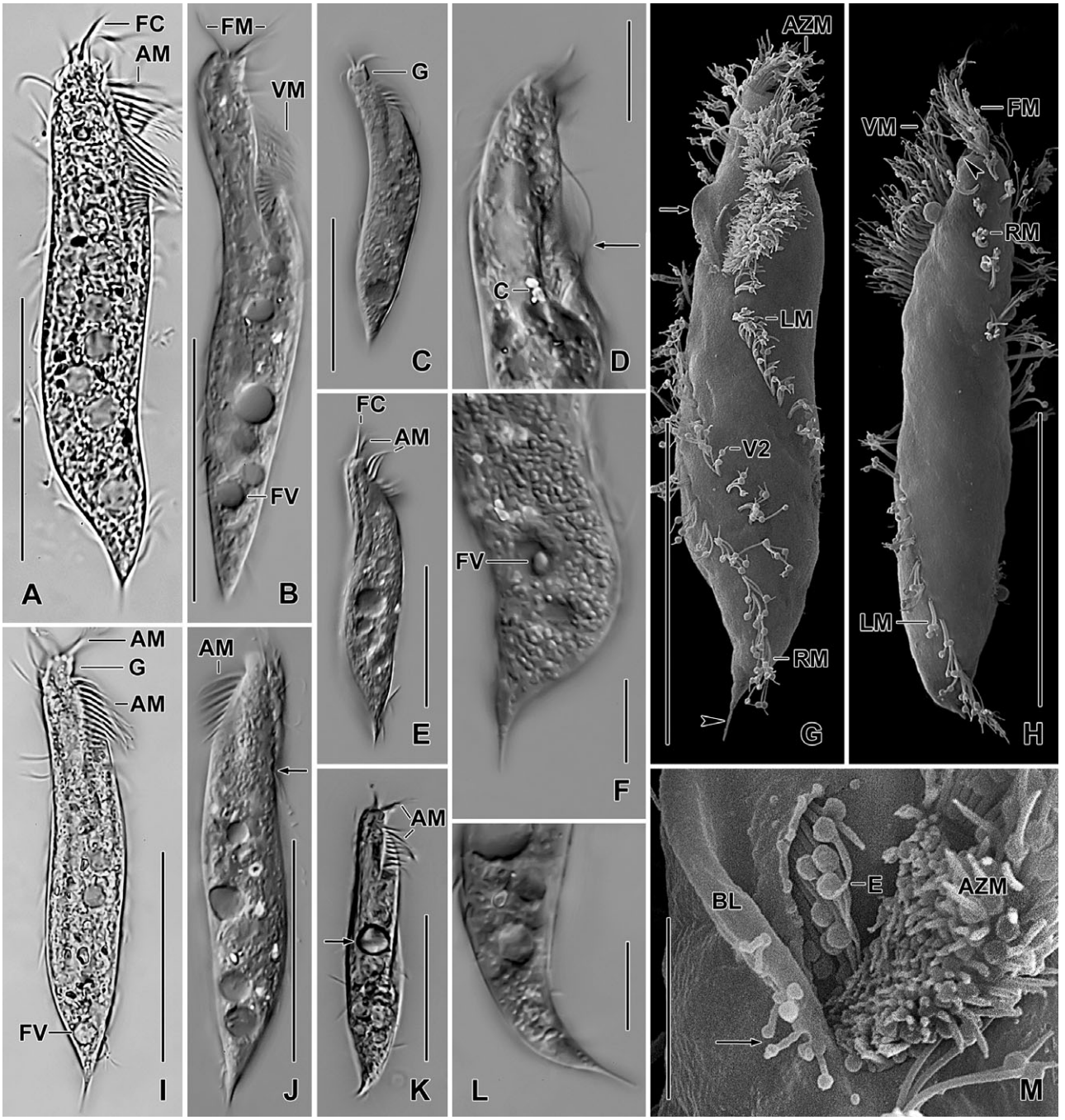

Figure 2 **(A–M)** *Schmidingerothrix salinarum* from life (A–F, I–L) and in the scanning electron microscope (G, H, M). **A–C, E, I, J.** Overviews of freely motile specimens, showing variability in body shape and cytoplasm. The arrow in Fig. J marks the right marginal row, which extends onto the dorsal side. Note the distinct gap (G) between frontal and ventral adoral membranelles (Fig. C, I); the acute posterior body end (Fig. I, J); and the food vacuoles (FV), most of which appear empty. **D.** Right side view of oral body portion, showing the conspicuous buccal lip (arrow; cp. with Fig. G). **F, L.** Posterior body region, showing the needle-shaped end and the granular cytoplasm (Fig. F). **G, H.** Ventral and dorsal view, showing the buccal lip (arrow), the acute posterior body end (arrowhead), and the absence of dorsal bristles (Fig. H). The arrowhead (Fig. H) marks the gap between ventral and frontal adoral membranelles. **K.** A small specimen, having ingested a starch grain (arrow) from the wheat kernels added to the culture. **M.** Posterior portion of oral apparatus, showing the endoral membrane (E) and the fringes on the posterior portion of the buccal lip (arrow). The globular structures associated with the lip fringes and the cilia are preparation artifacts. AM = adoral membranelles; AZM = adoral zone of membranelles; BL = buccal lip; C = cytoplasmic crystals; E = endoral membrane; FC = frontal cirri; FM = frontal adoral membranelles; FV = food vacuoles; G = gap between frontal and ventral adoral membranelles; LM = left marginal cirral row; RM = right marginal cirral row; VM = ventral adoral membranelles; V2 = ventral cirral row 2. Scale bars 5 μm (M), 10 μm (D, F, L), and 40 μm (A–C, E, G–K).

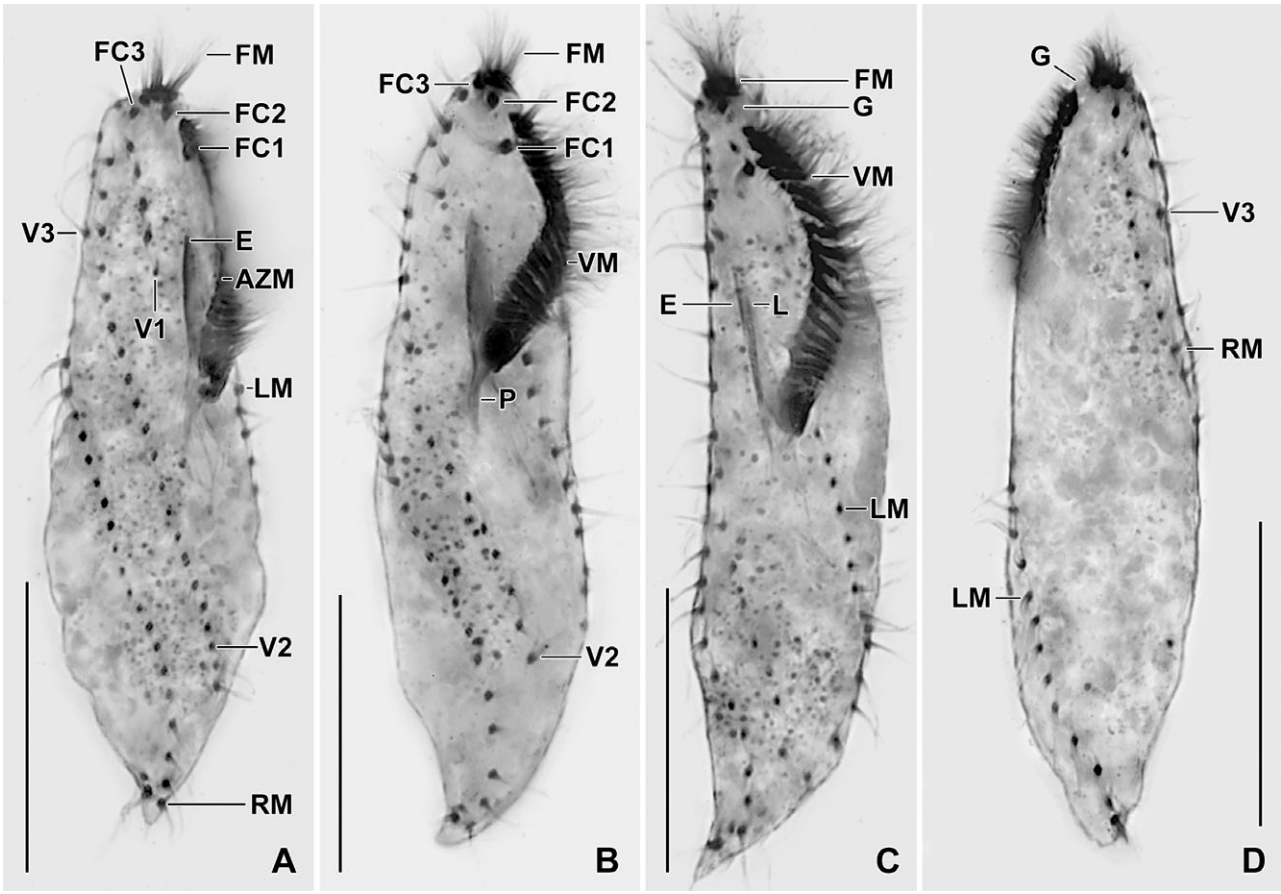

Figure 3 (**A–D**) *Schmidingerothrix salinarum*, infraciliature after protargol impregnation. The cells are slightly broadened due to the preparation procedures. **A, B.** Right side overviews. **C.** Ventral overview. **D.** Dorsal overview, showing the absence of bristle rows and the short ventral cirral row 3, which extends dorsolaterally and is thus difficult to recognize (Fig. A). AZM = adoral zone of membranelles; E = endoral membrane; FC1-3 = frontal cirri; FM = frontal adoral membranelles; G = gap between frontal and ventral adoral membranelles; L = buccal lip; LM = left marginal cirral row; P = pharyngeal fibers; RM = right marginal cirral row; VM = ventral adoral membranelles; V1-3 = ventral cirral rows. Scale bars 30 μm.

because the second is on the back (Fig. 1F, G, 4B; for typification, see Frankel 1989).

Molecular phylogeny (Fig. 5)

Using primer set EukA and EukB, we obtained a 1,769-base pairs-long fragment with a GC content of 45.11%. With significant support, the SSU rDNA sequence of *S. salinarum* is nested within the hypotrichs (Fig. 5). Both trees (NJ ED and ML) show *S. salinarum* as sister to a large clade mainly containing oxytrichid hypotrichs (support NJ ED: 94, support ML: 83). This "*Schmidingerothrix* clade" shows two subclades: the "*Oxytricha* subclade" has high bootstrap support (NJ ED: 97, ML: 97) while the "*Uroleptus* subclade" has poor support. Publicly available sequences, which are most closely related to the SSU rDNA sequence of *S. salinarum,* include those of *Bistichella variabilis* (GenBank accession number HQ699895 with 97.4% sequence similarity) and of *Orthoamphisiella breviseries* (GenBank accession number AY498654.1) with 97.2%. Both species belong to a clade within the *Uroleptus* subclade (support NJ ED: 77; no support from ML analysis).

Ontogenesis of *S. salinarum* (Fig. 6A–F, 7A–H, 8A–D)

The ontogenesis of *S. salinarum* is highly similar to that of *S. extraordinaria*, as described by Foissner (2012). Thus, we refer the reader to this article, to the figures cited above, and the few differences described in the next paragraph. Basically, the ontogenetic processes confirm the curious vegetative morphology, viz., the three-rowed adoral membranelles; the absence of a paroral membrane and of dorsal bristle rows; and of buccal, transverse, and caudal cirri. No vestiges of such structures are recognizable during ontogenesis. The division of the marginal cirral rows and of frontoventral cirral row 2 as well as of the nuclear apparatus and the cell occurs in the manner typical for hypotrichs (Fig. 6A–F, 7A–H, 8A–D). The tail of the proter and the gap between frontal and ventral adoral membranelles are completed in

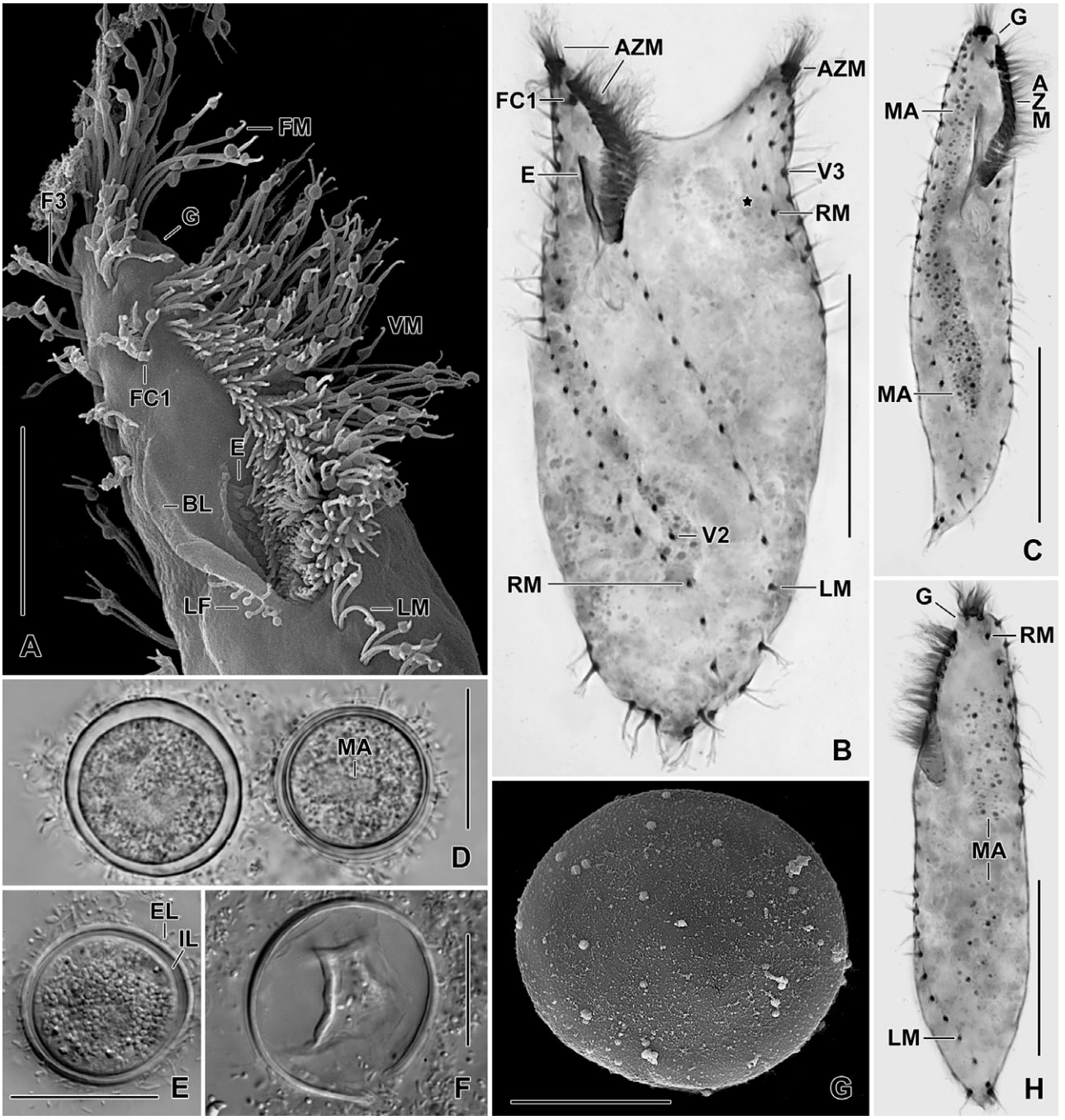

Figure 4 (**A**–**H**) *Schmidingerothrix salinarum* from life (D–F), after protargol impregnation (B, C, H), and in the scanning electron microscope (A, G). **A.** Ventral view of oral apparatus. Note the buccal lip fringes (LF), which are unique to the family Schmidingerotrichidae. The buccal cavity is covered by the buccal seal broken at the site of the endoral cilia. The globules associated with the lip fringes, the cirri, and the adoral cilia are preparation artifacts. **B.** About 2% of the cultivated specimens are homopolar doublets of type I, i.e., only one oral apparatus is visible because the second is on the backside (asterisk). **C, D.** The macronuclear nodules impregnate only faintly with the protargol method used. Note the gonostomoid adoral zone of membranelles in the specimen shown in Fig. C. **D**–**G.** The globular resting cysts have a smooth wall often covered with bacteria. The cyst wall is composed of an external layer and an internal layer, which disappears when the cyst contents are pressed out (Fig. F). The bright zone between external and internal layer is possibly the mesocyst. The macronuclear nodules are fused (Fig. D). AZM = adoral zone of membranelles; BL = buccal lip; E = endoral membrane; EL = external cyst layer; FC1-3 = frontal cirri; FM = frontal adoral membranelles; G = gap between frontal and ventral adoral membranelles; IL = inner cyst layer; LF = lip fringes; LM = left marginal cirral row; MA = macronuclear nodules; RM = right marginal cirral row; VM = ventral adoral membranelles; V2, 3 = ventral cirral rows. Scale bars 10 μm (A, G), 20 μm (D–F), and 30 μm (B, C, H).

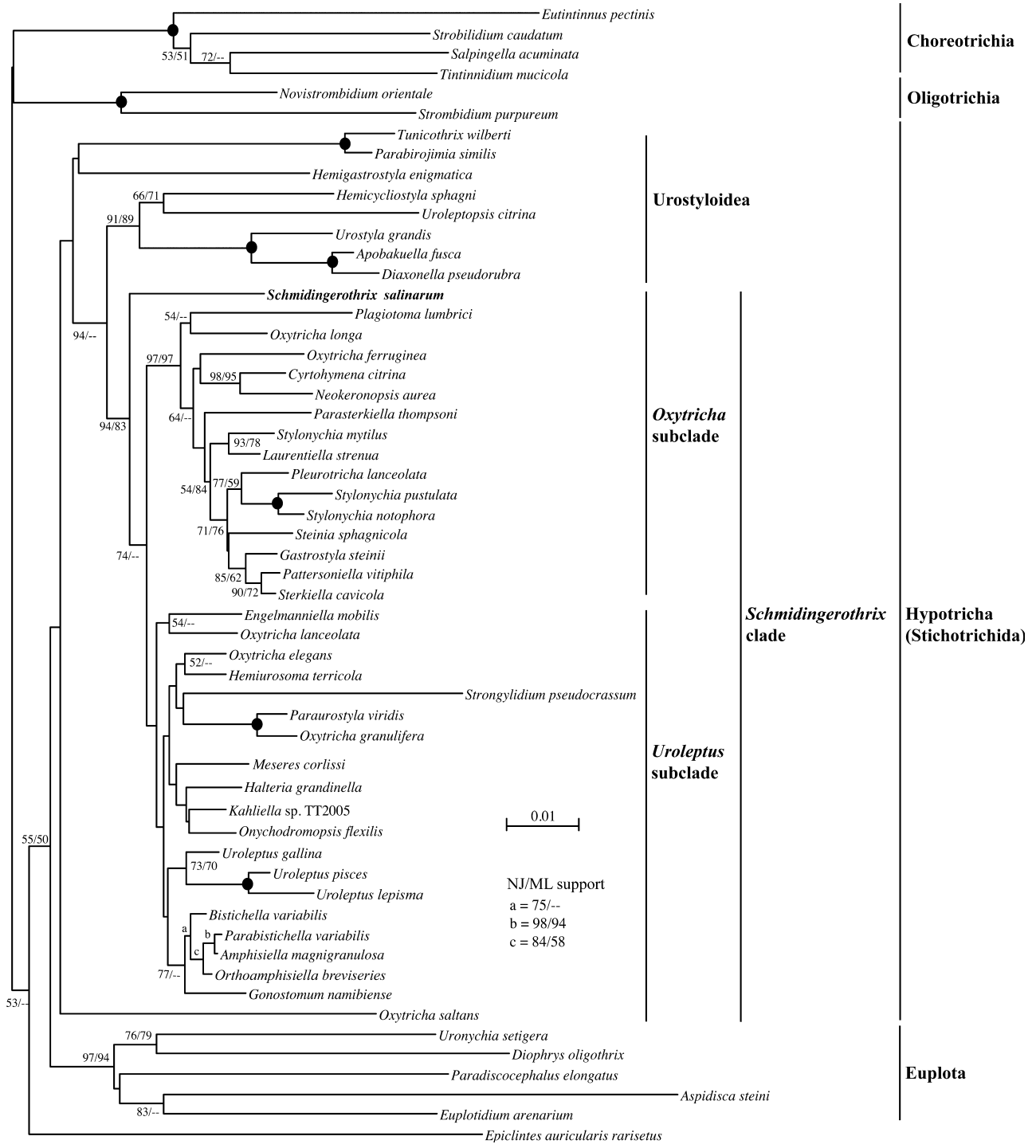

Figure 5 Maximum-likelihood tree of 18S rDNA sequences, showing the phylogenetic placement of *Schmidingerothrix salinarum*. The ciliate branches with significant support (NJ ED 94, ML 83) within the hypotrichs, basal to an *Oxytricha* subclade and an *Urolepus* subclade. Bootstrap values above 50 for the maximum-likelihood (ML, 100 replicates) and neighbor-joining evolutionary distance (1,000 replicates) analyses are given at the individual nodes. Black dots indicate 100% bootstrap support with both methods (first number ML, second number NJ). The edited sequence alignment includes 1,686 characters. The scale bar shows the substitution rate (0.01). Choreotrichia and Oligotrichia were chosen as outgroup. For details on tree construction, see Methods section.

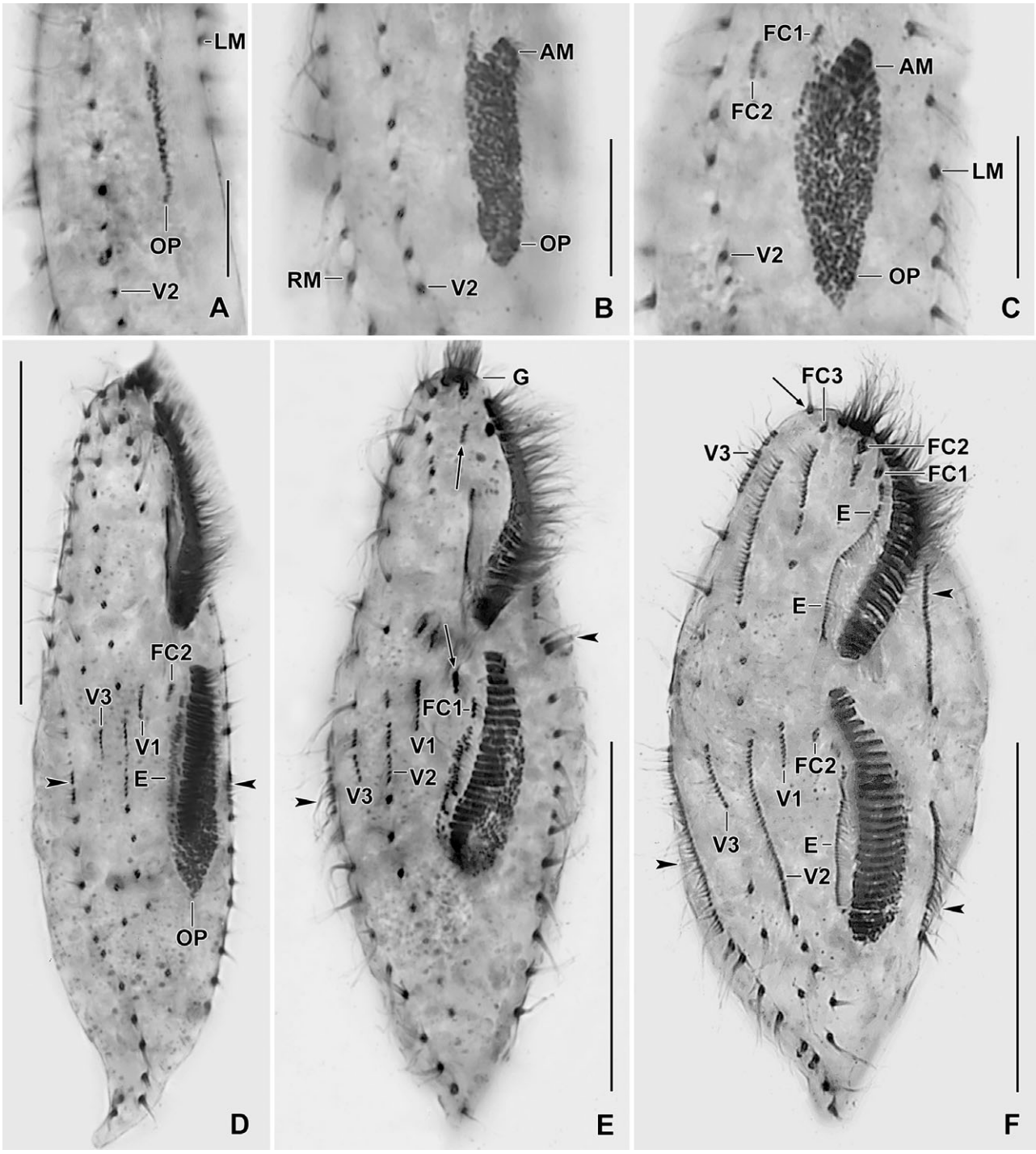

Figure 6 **(A-F)** *Schmidingerothrix salinarum*, ventral view of dividers after protargol impregnation. The arrowheads mark anlagen in the marginal cirral rows. **A.** Very early stage, showing the developing oral primordium posterior of the parental oral apparatus. **B, C.** Early stages, showing developing adoral membranelles and frontal cirri in the still growing oral primordium. **D.** A late early stage, showing anlagen only in the opisthe, where the endoral membrane is developing. **E.** Early mid-divider with anlagen in proter and opisthe. The second frontal cirrus develops de novo (arrows) in proter and opisthe. **F.** A mid-divider with distinct anlagen in proter and opisthe. In the proter, the parental frontal cirri are still present (FC1–3). The arrow marks the anterior most cirrus of the parental ventral row 3, where an anlage developed (V3). AM = adoral membranelles; E = endoral membrane; FC1-3 = frontal cirri; G = gap between frontal and ventral adoral membranelles; LM = left marginal cirral row; OP = oral primordium; RM = right marginal cirral row; V1-3 = ventral cirral rows. Scale bars 10 μm (A–C) and 40 μm (D–F).

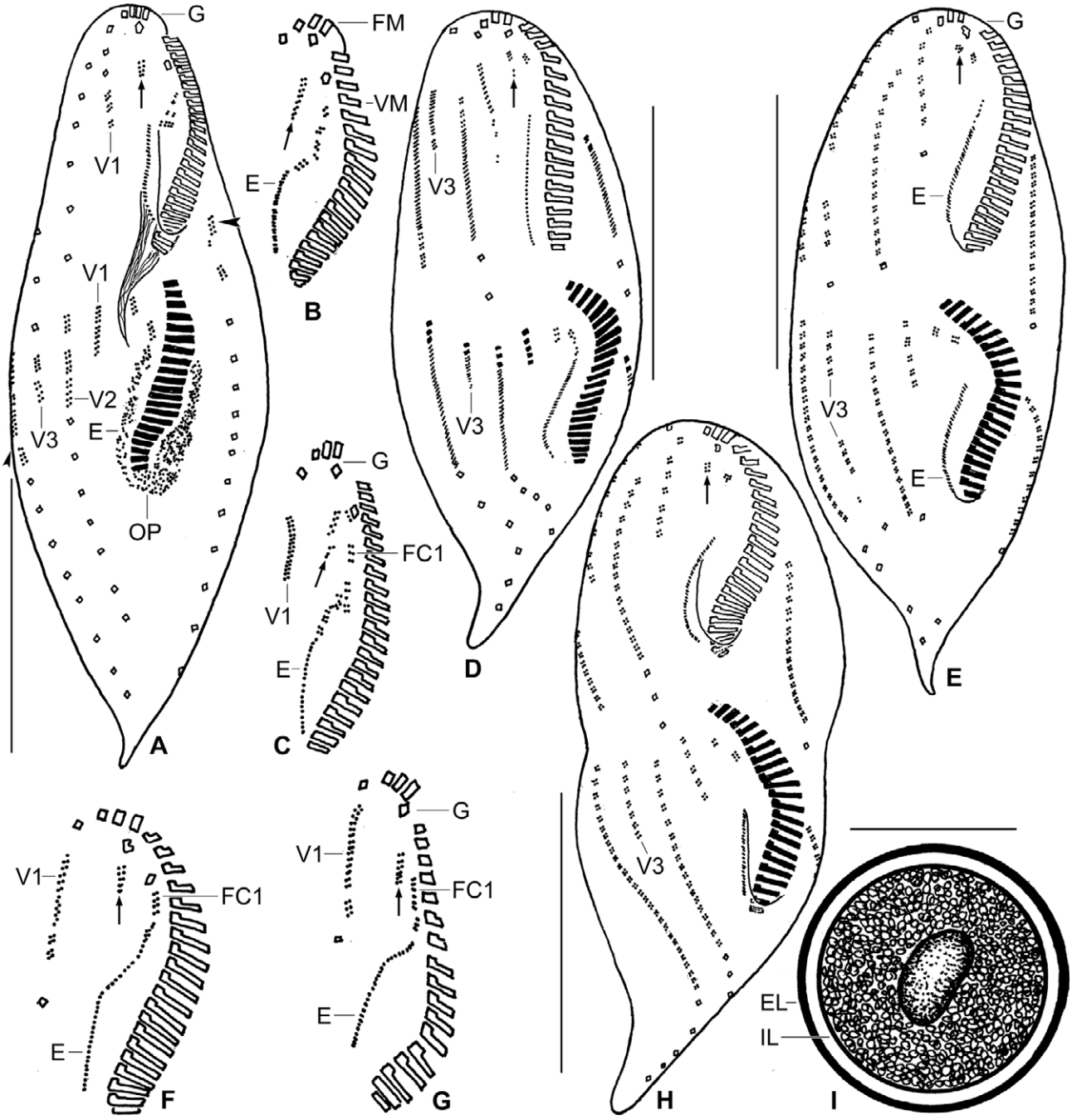

Figure 7 (**A–I**) *Schmidingerothrix salinarum*, ventral view of dividers after protargol impregnation (A–H) and a resting cyst in vivo (I). **A.** An early mid-divider, showing anlagen in the marginal cirral rows (arrowheads) and in frontoventral cirral row 1 of the proter. Frontal cirrus 2 (arrow) develops de novo in proter and opisthe. **B, C, F, G.** Development of frontal cirri in the proter. Frontal cirrus 1 (FC1) is generated by the parental endoral membrane, which produces basal bodies anteriorly. Frontal cirrus 2 originates de novo (arrows). Frontal cirrus 3 develops at the anterior end of frontoventral cirral row 1. **D.** A mid-divider with fully developed anlagen, producing cirri in the anterior region. The arrow marks the anlage for frontal cirrus 2. Frequently, the gap between frontal and ventral adoral membranelles disappears (Fig. D, F). **E.** A late mid-divider with new cirri in proter and opisthe. The arrow marks the new frontal cirrus 2. Note a split in frontoventral cirral row 3. **H.** A late divider with fully developed cirral pattern and commencing cell division. The arrow marks frontal cirrus 2. **I.** The wall of the resting cyst shows an external and an internal layer. The bright space between these layers might be the mesocyst. E = endoral membrane; EL = external cyst layer; FC1 = frontal cirrus 1; FM = frontal adoral membranelles; G = gap between frontal and ventral adoral membranelles; IL = internal cyst layer; OP = oral primordium; VM = ventral adoral membranelles; V1-3 = frontoventral cirral rows. Scale bars 20 μm (I) and 30 μm (A, D, E, H).

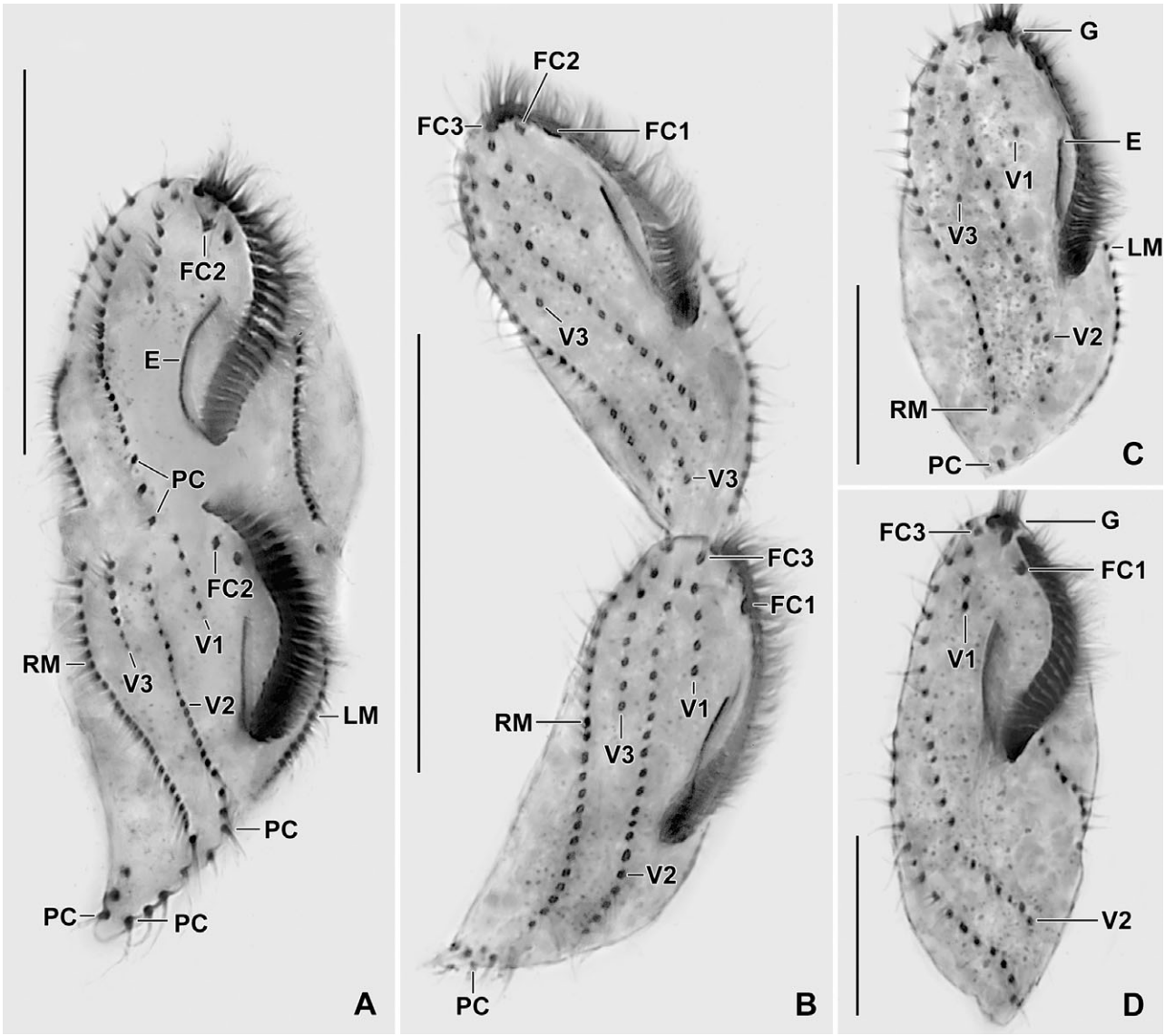

Figure 8 (**A-D**) *Schmidingerothrix salinarum*, ventral view of dividers (A, B), and postdividers (C, D) after protargol impregnation. **A.** A late divider with fully developed cirral pattern and beginning cell division. The gap between frontal and ventral adoral membranelles disappeared in the proter and has not yet developed in the opisthe. **B.** A very late divider with most parental cirri resorbed. Frontoventral cirral row 3 split in the proter. Frontal cirrus 2 is absent from the opisthe. **C, D.** A proter and an opisthe postdivider both developing the gap between frontal and ventral adoral membranelles. E = endoral membrane; FC1-3 = frontal cirri; G = gap between frontal and ventral adoral membranelles; LM = left marginal cirral row; PC = parental cirri; RM = right marginal cirral row; V1-3 = frontoventral cirral rows. Scale bars 20 μm (C, D) and 40 μm (A, B).

postdividers (Fig. 8C, D). All parental cirri not involved in anlagen formation are resorbed in late and very late dividers (Fig. 8A–D).

Frontal cirrus 1 is generated by the anlage for the undulating membranes both in proter and opisthe (Fig. 6E, 7A–H, 8A). The second frontal cirrus is generated de novo in both daughters, while the third frontal cirrus is produced by frontoventral cirral row 1 (Fig. 6D–F, 7A–H, 8A, B). The short frontoventral cirral rows 1 and 3 develop from the parental rows in the proter while de novo in the opisthe (Fig. 6D–F, 7A–H).

DISCUSSION

Comparison with *S. extraordinaria* and other hypotrichs

Schmidingerothrix salinarum differs from *S. extraordinaria* by three main features (cp. Fig. 1I, M): (i) three vs. one frontoventral cirral row; (ii) three vs. one frontal cirrus; and (iii) 24 vs. 18 adoral membranelles. Thus, these species are easily distinguished, especially by the number of frontoventral cirral rows.

There are many hypotrichs that superficially resemble *Schmidingerothrix* in vivo, for instance, most *Cladotricha* species (for a review, see Berger 2011). There is only one feature that defines *Schmidingerothrix* spp. unequivocally: the lack of dorsal bristles. Their absence or presence can be rather easily seen in vivo with interference contrast and in fixed material after protargol impregnation. Furthermore, *Schmidingerothrix* has a distinct molecular signature.

Ontogenesis

The ontogenesis of *S. salinarum* is quite similar to that of *S. extraordinaria*, as described by Foissner (2012). However, a direct comparison is difficult because the ciliature is much more reduced in the latter than the former (cf. Fig. 1I, M). Nonetheless, there is one distinct difference at least: frontal cirrus 1 is generated by the endoral membrane in *S. salinarum,* while it originates de novo in *S. extraordinaria*.

When compared with some supposed relatives, viz., *Cladotricha*, *Gonostomum,* and *Wallackia*, the ontogenesis is much less complex in *Schmidingerothrix*, especially the genesis of the undulating membranes and of anlagen I–III (for a review, see Berger 2011). Of special interest is *Cladotricha* that lacks a buccal cirrus and thus produces, as *Schmidingerothrix* (Fig. 6F, 7A–H), frontal cirrus 2 de novo (Borror and Evans 1979).

Classification of *Schmidingerothrix*

Foissner (2012) considered *Schmidingerothrix* as a secondarily oligomerized taxon because several typical hypotrich features are absent, especially the dorsal bristle rows and the paroral membrane. This hardly gets support from the molecular data, which show *Schmidingerothrix* as sister of a large clade containing typical oxytrichs (*Cyrtohymena*, *Sterkiella*, *Oxytricha*) and *Oxytricha*-like taxa such as *Hemiurosoma*, *Gonostomum*, and *Uroleptus* in which the midventral cirral pattern typical of urostylid hypotrichs evolved convergently (Foissner et al. 2004).

As mentioned above, several *Cladotricha* species are highly similar to *Schmidingerothrix* except that they have three rows of dorsal bristles, caudal cirri, and a minute paroral membrane highly reminiscent of that of *Halteria*, i.e., composed of only two cilia (Petz and Foissner 1992). Unfortunately, no sequence is available from *Cladotricha*, which, however, is morphologically rather similar to *Gonostomum* and *Kahliella* (for a review, see Berger 2011), showing a way how the *Uroleptus* subclade might have evolved from a *Schmidingerothrix*-like ancestor (Fig. 9).

The ground pattern of the Hypotricha

Berger (2008) suggested that the last common ancestor of the Hypotricha was similar to a present-day *Oxytricha*, i.e., had 18 fronto-ventral-transverse cirri, 2 marginal cirral rows, 3 rows of dorsal bristles, 3 caudal cirri, and 2 undulating membranes. Unfortunately, *Schmidingerothrix* is far from this pattern and thus cannot contribute to Berger's hypothesis. Furthermore, the urostylid clade diverges from the supposed oxytrichid ancestor earlier than *Schmidingerothrix*. Indeed, *Oxytricha saltans*, a marine species, is at the base of all hypotrichs but with low bootstrap support (Fig. 5).

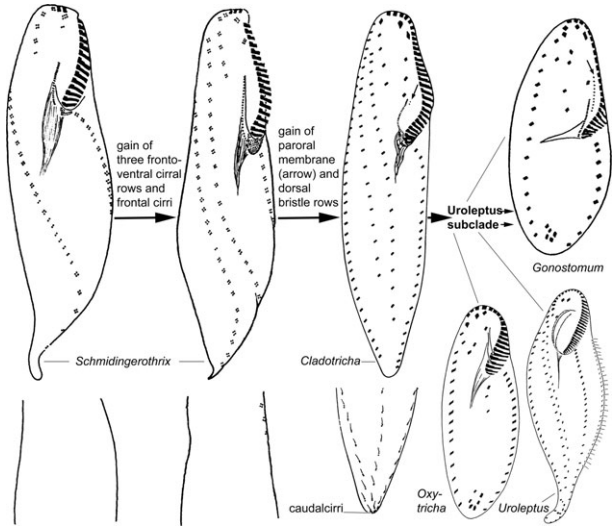

Figure 9 A phylogenetic scenario how the *Uroleptus* subclade could have evolved from a *Schmidingerothrix* ancestor via *Cladotricha*. Upper panel: ventral infraciliature, lower panel: dorsal infraciliature. Individual figures based on Berger (1999, 2006, 2008, 2011) and Foissner (2012).

If we assume an *Oxytricha*-like ancestor of the hypotrichs, then *Schmidingerothrix* could indeed be a heavily oligomerized taxon that later reactivated the basal *Oxytricha* pattern via a *Cladotricha*-like stage.

TAXONOMIC SUMMARY

Class Spirotrichea Buetschli 1889
Subclass Hypotricha Stein 1859
Order Stichotrichida Fauré-Fremiet 1961
Family Schmidingerotrichidae Foissner 2012
Genus *Schmidingerothrix* Foissner 2012
Species *Schmidingerothrix salinarum* n. spec.

Diagnosis

Size in vivo about 95 × 17 μm. Body slender (~5.5:1), usually widest in mid-portion, with short but distinct tail. Four macronuclear nodules, forming a series near right margin of cell; zero to two micronuclei. Cortical granules in loose rows, colorless, about 1 μm across. Three frontal cirri and three frontoventral cirral rows. Frontal cirrus 1 subapical close to ventral part of adoral zone of membranelles. Frontoventral row 1 composed of an average of four cirri; row 2 of 18 cirri, row 3 of five cirri. Right marginal row composed of an average of 23 cirri, left of 17. Adoral zone about 32% of body length, composed of an average of three frontal and 21 ventral membranelles. Endoral membrane 12 μm long on average.

Type locality

Solar saltern in the Ria Formosa National Park near to the town of Faro, Portugal (N37°0′29.4851″, W7°57′ 41.0684″).

Type material

One holotype and two paratype slides with protargol-impregnated specimens and two paratype slides with hematoxylin-stained cells have been deposited in the Biologiezentrum of the Oberösterreichische Landesmuseum in Linz (LI), Austria, reg. no. 2013/33-37. Relevant specimens have been marked by black ink circles on the coverslip. Gen-Bank accession number: KC991098.

Etymology

The species name is a noun in plural genitive and thus does not change the gender when combined with, e.g., a masculine genus; it refers to the environment, i.e., growing or living in highly saline habitats.

ACKNOWLEDGMENTS

Financial support was provided by the Austrian Science Fund (FWF, project P22846-B17), the German Science Fund (DFG, STO414/3-2), and ASSEMBLE with a grant to TS and SF. We gratefully acknowledge the technical assistance of Mag. Barbara Komm, Johannes Rattey M.Sc., Robert Schörghofer, Andreas Zankl, and Hans-Werner Breiner and the staff of CCMAR (Faro, Portugal) for support during field work.

LITERATURE CITED

Adam, H. & Czihak, G. 1964. Arbeitsmethoden der makroskopischen und mikroskopischen Anatomie. G. Fischer, Stuttgart. 583 p.

Berger, H. 1999. Monograph of the Oxytrichidae (Ciliophora Hypotrichia). *Monographiae Biol.*, 78(i-xiii):1–1080.

Berger, H. 2006. Monograph of the Urostyloidea (Ciliophora Hypotricha). *Monographiae Biol.*, 85(i-xvi):1–1303.

Berger, H. 2008. Monograph of the Amphisiellidae and Trachelostylidae (Ciliophora Hypotricha). *Monographiae Biol.*, 88(i-xiii):1–737.

Berger, H. 2011. Monograph of the Gonostomatidae and Kahliellidae (Ciliophora Hypotricha). *Monographiae Biol.*, 90(i-xiv):1–741.

Borror, A. C. & Evans, F. R. 1979. *Cladotricha* and phylogeny in the suborder Stichotrichina (Ciliophora, Hypotrichida). *J. Protozool.*, 26:51–55.

Buetschli, O. 1889. Protozoa. III. Abtheilung: Infusoria und System der Radiolaria. *In*: Bronn, H. G. (ed.), Klassen und Ordnungen des Thier-Reichs, wissenschaftlich dargestellt in Wort und Bild, Erster Band. Winter, Leipzig. p. 1585–2035.

Castresana, J. 2000. Selection of conserved blocks from multiple alignments for their use in phylogenetic analysis. *Mol. Biol. Evol.*, 17:540–552.

Crisp, M. D. & Cook, L. G. 2005. Do early branching lineages signify ancestral traits?. *Trends Ecol. Evol.*, 20:122–128.

Edgar, R. C. 2004. MUSCLE: a multiple sequence alignment method with reduced time and space complexity. *BMC Bioinformatics*, 5:113.

Fauré-Fremiet, E. 1961. Remarques sur la morphologie comparée et la systématique des ciliata Hypotrichida. *C. r. hebd. Séanc. Acad. Sci. Paris*, 252:3515–3519.

Foissner, W. 2012. *Schmidingerothrix extraordinaria* nov. gen., nov. spec., a secondarily oligomerized hypotrich (Ciliophora, Hypotricha, Schmidingerotrichidae nov. fam.) from hypersaline soils of Africa. *Eur. J. Protistol.*, 48:237–251.

Foissner, W. & Al-Rasheid, K. 2006. A unified organization of the stichotrichine oral apparatus, including a description of the buccal seal (Ciliophora: Spirotrichea). *Acta Protozool.*, 45:1–16.

Foissner, W. & Stoeck, T. 2011. *Cotterillia bromelicola* nov. gen., nov. spec., a gonostomatid ciliate (Ciliophora, Hypotricha) from tank bromeliads (Bromeliaceae) with de novo originating dorsal kineties. *Eur. J. Protistol.*, 47:29–50.

Foissner, W., Moon-van der Staay, S. Y., van der Staay, G. W. M., Hackstein, J. H. P., Krautgartner, W.-D. & Berger, H. 2004. Reconciling classical and molecular phylogenies in the stichotrichines (Ciliophora, Spirotrichea), including new sequences from some rare species. *Eur. J. Protistol.*, 40:265–281.

Frankel, J. 1989. Pattern Formation. Ciliate Studies and Models. Oxford University Press, New York, Oxford. p. (i–ix), 1–314.

Galtier, N., Gouy, M. & Gautier, C. 1996. SEAVIEW and PHYLO_WIN: two graphic tools for sequence alignment and molecular phylogeny. *Comput. Appl. Biosci.*, 12:543–548.

Guindon, S. & Gascuel, O. 2003. A simple, fast, accurate algorithm to estimate large phylogenies by maximum likelihood. *Syst. Biol.*, 52:696–704.

Hu, X., Hu, X., Al-Rasheid, K. A. S., Al-Farraj, S. A. & Song, W. 2011. Insights into the phylogeny of sporadotrichid ciliates (Protozoa, Ciliophora: Hypotricha) based on genealogical analyses of multiple molecular markers. *Chin. J. Oceanol. Limnol.*, 29:96–102.

Krell, F.-T. & Cranston, P. S. 2004. Which side of the tree is more basal? *System. Entomol.*, 29:279–281.

Liu, W., Shao, C., Gong, J., Li, J., Lin, X. & Song, W. 2010. Morphology, morphogenesis and molecular phylogeny of a new marine urostylid ciliate (Ciliophora, Stichotrichia) from the South China Sea, and an overview of the convergent evolution of the midventral complex within the Spirotrichea. *Zool. J. Linn. Soc.*, 158:697–710.

Lynn, D. H. 2008. The Ciliated Protozoa. Characterization, Classification and Guide to the Literature, 3rd ed. Springer, Dordrecht. p. (i–xxxii), 1–605.

Medlin, L., Elwood, H. J., Stickel, S. & Sogin, M. L. 1988. The characterization of enzymatically amplified eukaryotic 16S-like rRNA-coding regions. *Gene*, 71:491–499.

Paiva, T. S., Borges, B. N., Harada, M. L. & Silva-Neto, I. D. 2009. Comparative phylogenetic study of Stichotrichia (Alveolata: Ciliophora: Spirotrichea) based on 18S-rDNA sequences. *Genet. Mol. Res.*, 8:223–246.

Petz, W. & Foissner, W. 1992. Morphology and morphogenesis of *Strobilidium caudatum* (Fromentel) *Meseres corlissi* n. sp., *Halteria grandinella* (Müller), and *Strombidium rehwaldi* n. sp., and a proposed phylogenetic system for oligotrich ciliates (Protozoa, Ciliophora). *J. Protozool.*, 39:159–176.

Posada, D. 2008. jModelTest: phylogenetic model averaging. *Mol. Biol. Evol.*, 25:1253–1256.

Schmidt, S. L., Bernhard, D., Schlegel, M. & Foissner, W. 2007. Phylogeny of the Stichotrichia (Ciliophora; Spirotrichea) reconstructed with nuclear small subunit rRNA gene sequences: discrepancies and accordances with morphological data. *J. Eukaryot. Microbiol.*, 54:201–209.

Stamatakis, A., Hoover, P. & Rougemont, J. 2008. A fast bootstrapping algorithm for the RAxML web-servers. *Syst. Biol.*, 57:758–771.

Stein, F. 1859. Der Organismus der Infusionsthiere nach eigenen Forschungen in systematischer Reihenfolge bearbeitet. I. Abtheilung. Allgemeiner Theil und Naturgeschichte der hypotrichen Infusionsthiere. Engelmann, Leipzig, p. (i–xii), 1–605.

Vd'ačný, P. & Foissner, W. 2012. Monograph of the Dileptids (Protista, Ciliophora, Rhynchostomatia). *Denisia*, 31:1–529.